The influences of catchment geomorphology and scale on runoff generation in a northern peatland complex

Murray Richardson,[1]* Scott Ketcheson,[2] Peter Whittington[2] and Jonathan Price[2]

[1] *Department of Geography and Environmental Studies, Carleton University, 1125 Colonel By Dr., Ottawa, ON, Canada, K1S 5B6*
[2] *Department of Geography and Environmental Management, University of Waterloo, 200 University Ave, Waterloo, ON, Canada, N2L 3G1*

Abstract:

We computed daily discharge (Q) *versus* gross drainage area (GDA) regression analyses for the 2009 and 2010 growing seasons for six small to medium headwater catchments at a northern peatland complex in the James/Hudson Bay lowlands. Temporal dynamics of the daily goodness of fits (R^2) between Q and GDA were then examined to identify the most relevant conceptual model of runoff generation in this landscape. We observed high R^2 values during low flow conditions (mean $R^2 = 0.93$ for 2009 and 2010). During wetter periods and in particular during large runoff events, the relationship degraded rapidly and consistently, suggesting differences in quickflow response among the gauged catchments. At low flows, the six catchments generated equivalent amounts of runoff (mm), leading to a strong Q–GDA relationship. During high flows, total growing season runoff increased systematically with GDA between 8 and 50 km^2 and then decreased with further increases in GDA. These differences were responsible for the observed breakdown in the daily Q–GDA relationships and also resulted in significant differences in total runoff among the six catchments during the wetter year. Quantitative landscape analysis using a 5-m resolution Light Detection and Ranging (LiDAR) digital elevation model revealed that near-stream zone characteristics vary systematically with scale in a manner that is consistent with the observed patterns of quickflow runoff response. In this northern peatland complex, fast-responding flowpaths in the spatially discrete near-stream zones may be the key determinant of catchment runoff efficiency at the small to medium (~10 to ~200 km^2) headwater catchment scales analysed here. Moreover, the relatively organized drainage patterns observed in this study are consistent with our understanding of ecohydrological feedbacks driving geomorphic evolution of northern peatlands. Copyright © 2012 John Wiley & Sons, Ltd.

KEY WORDS   catchment hydrology; watershed; runoff; scaling; LiDAR; wetlands; variable source area (VSA); lowlands; topographic wetness index

Received 18 August 2011; Accepted 6 March 2012

INTRODUCTION

The Hudson Bay Lowlands (HBL) ecozone in northern Ontario, Canada, represents one fourth of the province's terrestrial landmass and is a significant source of freshwater to the saline James Bay (Rouse *et al.*, 1992). Runoff generating processes in low gradient northern landscapes such as HBL are poorly understood; however, new capacity for hydrologic prediction in ungauged peatland basins of Canada is urgently required (Whitfield *et al.*, 2009). The HBL supports the largest wetland complex in North America with more than 85% areal composition of either minerotrophic wetland or organic peatland, arranged in complex mosaics of bogs, fens, swamps and permafrost plateaus (Riley, 2011). It not only is an ecosystem of global ecological significance but also comprises a vast area of mineral and energy deposits and thus faces numerous current or imminent resource development pressures. The region is undergoing an unprecedented period of rapid climate change (Gough and Wolfe, 2001; Gagnon and Gough, 2005), and corresponding ecological changes are widely expected or already underway (Riley, 2011). Additional efforts are required to improve current scientific understanding of hydrologic and biogeochemical regimes in the HBL to help predict future impacts of resource development and climate change in this important ecoregion of Canada (Riley, 2011).

Much recent progress has been made towards understanding water cycle dynamics and physical mechanisms of water flow in northern peatlands of Canada (Waddington *et al.*, 2009). One poorly understood aspect of northern peatland hydrology, however, is how lateral movement of water within and between distinct landcover types interact to produce catchment scale runoff dynamics. As a result, storage and routing processes are thought to be an important source of error in physically based numerical models of northern peatland hydrology (Quinton *et al.*, 2003). There is a growing appreciation for the role of discrete landscape units in governing whole-catchment rainfall–runoff response in northern regions of Canada (Spence, 2010; Oswald *et al.*, 2011; Phillips *et al.*, 2011), and past research suggests that similar mechanisms apply in peatland basins (Quinton and Roulet, 1998; Quinton *et al.*, 2003). In particular, Quinton and Roulet (1998) found that transient connectivity along pool-ridge complexes in a subarctic channel fen immediately adjacent to the outlet of a 24.2 ha

*Correspondence to: Murray Richardson, Department of Geography and Environmental Studies, Carleton University, 1125 Colonel By Dr., Ottawa, ON, Canada, K1S 5B6.
E-mail: murray_richardson@carleton.ca*

catchment could largely explain the observed hydrograph response. Subsequent work by Quinton *et al.* (2003) demonstrated the importance of landcover type (i.e. bog *vs* fen) in governing mean annual runoff in mesoscale (150–2000 km^2) peatland dominated basins in a continental high boreal region of Canada. However, there is a need to bridge the analysis scales represented by these two important studies to help increase our understanding of runoff generating mechanisms in headwater to mesoscale catchments (e.g. ~1–100 km^2) to improve the predictive capacity in peatland basins.

To this end, scaling studies focused on runoff generation in other regions of the world offer a promising strategy that has not been explored in northern peatland basins. Investigations into runoff generation across scales provide insight into first-order controls on catchment hydrology and rainfall–runoff response, particularly if the observed scaling behaviour can be linked to quantifiable metrics of landscape physiography or geomorphology (McGlynn *et al.*, 2003; McGlynn *et al.*, 2004; McGuire *et al.*, 2005; Buttle and Eimers, 2009). Such linkages can be used to improve parameterization of hydrological models for ungauged basins (Buttle and Eimers, 2009).

The simplest example of a quantifiable scaling relationship in hydrology is that between mean annual streamflow and drainage area, which can be used to pro-rate flows for ungauged basins on the basis of nearby gauged basins. Other streamflow metrics (e.g. runoff coefficients, peak runoff and lag-to-peak) may or may not vary predictably with drainage area, and the degree to which such relationships exist may reflect differences in landcover proportions and/or runoff generating mechanisms with scale. McGlynn *et al.* (2004) conducted a simultaneous assessment of the effects of catchment size and landscape structure on runoff processes in the Maimai research catchments, New Zealand, which are mountainous, highly dissected systems that exhibit very well-organized drainage patterns. They identified riparian headwater areas to be consistent contributors to catchment scale event runoff, whereas valley bottom areas further downstream were not, depending on antecedent wetness conditions, event size and associated influences on hydrologic connectivity between these landscape units and adjacent stream segments. Past work in these research catchments has also demonstrated that riparian widths exhibit clear and consistent scaling behaviour, increasing in width with catchment area (McGlynn and Seibert, 2003), which corroborates the observed runoff scaling behaviour in these catchments. Catchment geomorphology, which evolves slowly over decades to millennia in response to climate, geology, hydrology and vegetation dynamics, imparts strong controls on contemporary hydrologic regimes (Beven *et al.*, 1988; Troch *et al.*, 1995; McGlynn *et al.*, 2003; Woods, 2003; McGuire *et al.*, 2005; Thompson *et al.*, 2011). It can, therefore, provide important insight into processes driving catchment hydrological dynamics and scaling behaviours. This concept has driven many key hydrologic modelling developments in the past, including the geomorphic instantaneous unit hydrograph approach (Rodriguez-Iturbe and Valdes, 1979) and TOPMODEL (Beven and Kirkby, 1979).

Peatlands are complex, adaptive ecosystems where water plays a fundamental role in physical and biological feedbacks controlling geomorphic form and ecological function (Clymo, 1984; Damman, 1986). In the northern lowland regions of Ontario and Canada, peatlands are the dominant landcover, and wetland ecohydrology, catchment geomorphology and runoff generation are inextricably linked through complex feedback mechanisms operating simultaneously across multiple spatial and temporal scales. Recent efforts to better understand northern peatland geomorphology and development in the HBL highlight the importance of the combined influences of hydrology and geology in driving peatland succession (Glaser *et al.*, 2004). Similarly, Watters and Stanley (2007) point to both physical and biological drivers of stream geomorphology in a northern Wisconsin peatland basin. There is evidence to suggest, therefore, that landscape evolution in northern peatland catchments leads to well-organized and thus potentially predictable geomorphic structure and scaling relationships. Nevertheless, relatively little progress has been made in linking catchment geomorphology to runoff processes in northern peatland basins. Examining the effects of catchment size and landscape structure on runoff generation in northern peatlands may therefore improve our understanding of lowland hydrology and lead to improved capacity for operational prediction in ungauged basins of this region.

Given the various concerns over northern peatland ecosystems and the need for better predictive models of lowland hydrology, the present study was initiated to assess relationships between catchment geomorphology, scale and runoff generation at a James Bay Lowland research site in the HBL ecozone of northern Ontario, Canada. The specific objectives were to (1) assess how runoff timing and magnitude varies with catchment size in a northern peatland complex; (2) determine whether several quantitative metrics of catchment morphology derived from a high resolution digital elevation model (DEM) vary with spatial scale in this region; and (3) assess whether observed runoff and geomorphic scaling relationships are consistent with one another, thus providing insight into first-order controls on runoff generation in northern peatland catchments.

STUDY SITE

The study site (Figure 1) is located in the vicinity of the De Beers Victor Diamond Mine 500 km north-northwest of Timmins, Ontario; 90-km west of Attawapiskat, Ontario, in the James Bay Lowland ecoregion of the HBL ecozone (52.83°N, 83.93°W) and falls within a zone of 'sporadic discontinuous permafrost' (Riley, 2011). Six gauged, medium to large headwater catchments (Strahler stream orders 1–4) with a combined area of 441 km^2 and ranging in size from 8 to 200 km^2 were included in the analyses (Figure 1). The landscape comprises an assortment of bog and fen subtypes typical of James Bay lowland
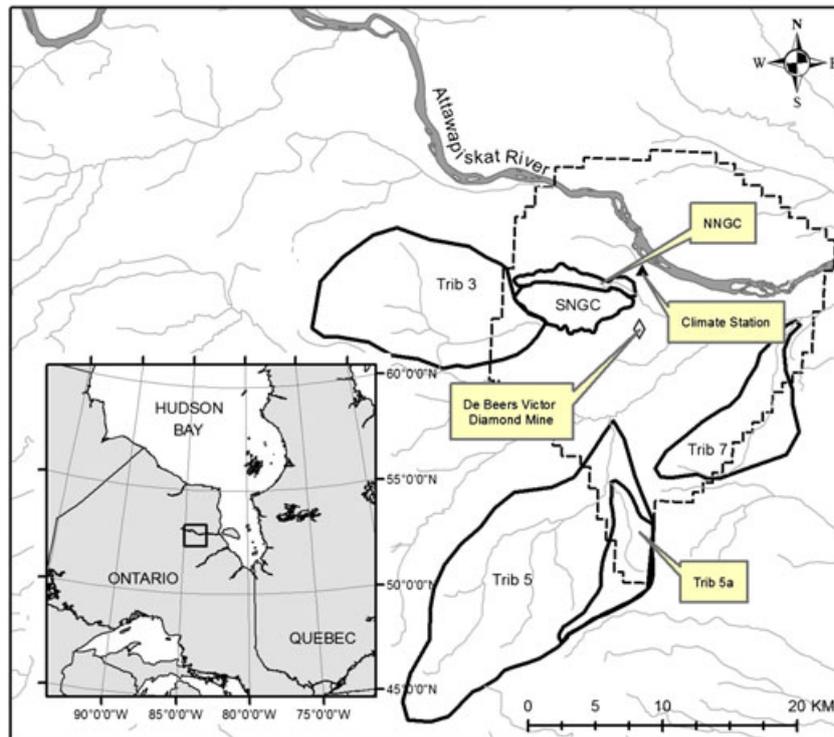
Figure 1. Study area surrounding the De Beers Victor Diamond Mine in the James Bay lowland ecoregion of the HBL, northern Ontario, Canada, showing catchment boundaries and national stream hydrography layer. Landscape analysis was conducted within the LiDAR footprint only (dashed line). NNGC = 'North-North Granny Creek' and SNGC = 'South-North Granny Creek'

regions (Riley, 2011), which, when combined with open water classes, cover more than 90% of the landscape. Drainage networks in headwater systems are predominantly channel fens or fen water tracks. Along the fen water tracks, channels are intermittent to non-existent, but during periods of high flow or during the freshet when frozen ground is prevalent, overland flow between small pools can be observed. The two closest stations with long-term meteorological records are Lansdowne House (inland 300 km west-southwest) and Moosonee (near the coast, 250 km south-east). The average annual January and July temperatures for Lansdowne House are −22.3 and 17.2 °C, respectively, and for Moosonee are −20.7 and 15.4 °C, respectively (Environment Canada, 2003). Annual precipitation for Lansdowne House is 700 mm with ~35% falling as snow; for Moosonee, precipitation is 682 mm with ~31% falling as snow. Evapotranspiration is 431 mm year^{-1} (Singer and Chen, 2002). In a typical year, therefore, surplus precipitation is approximately 270 mm. The open-pit diamond mining operations require substantial groundwater pumping to dewater the mine and are causing depressurization of the regional bedrock aquifer. In late 2011, the 2-m drawdown contour in the upper bedrock occupied less than 10% of the combined area of the North-North Granny Creek and South-North Granny Creek catchments and would have been even less in 2009/2010. Recent work has quantified the vertical connection in 'well-connected' areas (i.e. bedrock close to or at the surface) (Whittington and Price, 2012) as well as those areas with thick marine sediments (unpublished data) and found that the associated seepage loss across the entire watershed was less than 5% of the total annual precipitation. This amount is

well within the measurement error of water flux components presented in the current study and was ruled out as having any significant impact on the results and interpretation.

METHODS

Hydrometric data collection

Continuous streamflow discharge measurements were made between 5 May and 15 October in 2009 and 2010, for six catchments spanning three orders of magnitude (8–200 km^2). Open channel flow gauging stations were established for spot discharge measurements using a YSI (Yellow Springs, Ohio, USA) Flowtracker Acoustic Doppler Velocimeter. Hourly stage measurements were logged using Schlumberger (Kitchener, Ontario, Canada) Diver water level logging pressure transducers, housed in slotted 2.5-cm diameter PVC stand pipes. For each site, a stage–discharge relationship was established and used to convert hourly stage measurements to discharge. At some sites, the stage–discharge relationships were re-established annually to account for shifts in the relationship caused by changes in channel morphology. Hourly flows were converted to daily flows for the purposes of all subsequent analyses. A meteorological tower was instrumented ~2-km north-west of the mine site and measured precipitation, temperature, relative humidity, net radiation, wind speed and direction connected to a CS1000 data logger and recorded every 10 min.

Runoff analysis

The 2009 and 2010 streamflow records were analysed to assess daily variations in the relationship between

discharge and gross drainage area (*GDA*). Winter and early spring freshet periods were omitted because of ice damming effects on stage−discharge relationships. To calculate *GDA*s, catchment boundaries were digitized on-screen using ArcGIS software (ESRI, 2011) by manually interpreting drainage networks and divides using Bing Maps Aerial imagery, available to licenced ESRI software users. This imagery was of sufficiently high resolution that drainage networks were readily visible and catchment divides inferred more accurately than what was deemed to be possible using Canadian National Topographic Database 1 : 50 000 scale hydrography layers. Interpretation of flow systems and catchment areas in this manner was straightforward, facilitated by the abundance of surface water and knowledge of peatland forms, in particular fen water tracks from which flow direction can be judged, and bogs on the interfluves that assist in defining basin boundaries. *GDA* for each catchment outlet was then calculated from the digitized polygon features. With the use of these derived areas, a daily regression of discharge (*Q*) ($m^3 s^{-1}$) *versus GDA* was computed with a custom script in the R statistical software (R Development Core Team, 2009), and the resulting daily coefficient of determination (R^2) was plotted to show a time series of the strength of the relationship between *Q* and *GDA*. Runoff from each of the study catchments was also plotted to identify temporal variability in the strength of this relationship and to use this as a metric to assess similarities or differences in runoff generating processes across scale. The use of runoff (mm) rather than *Q* plots standardizes for catchment areas, facilitating the interpretation of inter-catchment differences in runoff generation. Overall, the *Q–GDA* approach was used to assess the applicability of two prevailing conceptual models of runoff generation, namely the variable source area (VSA) theory and the emerging paradigm of landscape element threshold regimes ('fill-and-spill') thought to predominate in other regions of Canada and the world where depression storage (e.g. lakes and wetlands) can be large (Stichling and Blackwell, 1958; Quinton and Roulet, 1998; Spence, 2010; Oswald *et al.*, 2011). Specifically, it was hypothesized that the strength of *Q–GDA* relationship would exhibit strong temporal variability because of differences in either the timing or magnitude of runoff generation. For example, previous work has shown that runoff generation in shield landscapes is strongly coupled to areal extent and connectivity of active contributing areas and that runoff efficiency of shield catchments is strongly hysteretic in relation to catchment storage because of the storage dynamics of lakes and wetlands along the drainage network (Phillips *et al.*, 2011). Hysteresis, nonlinear storage thresholds and temporally varying connectivity of active contributing areas were all considered as factors that might lead to temporal variations in the strength of the daily *Q–GDA* relationship. Our objective, therefore, was to use the temporal analysis of the strength of the *Q–GDA* relationship to gain insight into inter-catchment differences in runoff generating processes and, if possible, to attribute these to differences in catchment geomorphology and/or scale.

Catchment-specific analyses were also conducted on the runoff data. Discharge hydrographs were converted to runoff (mm) using the derived *GDA*s. Daily runoff was analysed for each catchment during low, medium and high flow conditions. The classification of these flow periods was based on the mean daily runoff for all six catchments. Low flow periods were those days falling within the bottom 10% of the ranked distribution of mean daily flows. Medium flow condition days were considered to be any days falling between the 55th and 65th percentiles, and high flow days were considered to be any days on which mean daily flows were ≥90th percentile. Note that these percentiles were computed separately for each year. Paired Wilcoxon rank sum tests were conducted for each catchment pair for daily runoff to determine the statistical significance of observed differences in total runoff from each catchment in 2009 and 2010 (H_0 : mean pair-wise difference of daily runoff = 0 mm).

LiDAR acquisition and DEM interpolation

A discrete-return airborne LiDAR survey was conducted in July 2007 by Terrapoint Canada Inc. over a 462 km^2 area encompassing a portion of the study area, shown in Figure 1. Laser pulse returns were classified into bare earth and vegetation classes by Terrapoint and delivered as tiled, xyz ASCII files. The nominal density of bare earth returns was 0.5 points per m^2 ground surface. A 5-m pixel resolution DEM was interpolated from the classified bare earth returns using an inverse distance weighted interpolator with a low weighting exponent (0.5) and a maximum of four neighbouring points. A DEM resolution of 5 m was found to offer a reasonable balance between computational efficiency and topographic detail. An accuracy assessment was conducted on the basis of approximately 350 wetland ground surface elevations surveyed along a 1500 m research transect using a Topcon (Tokyo, Japan) HiPER GL RTK GPS system. The root mean square error was determined to be 2.5 cm for surveyed *versus* LiDAR-derived elevations interpolated to 5-m grid spacing using the same parameters listed previously. This level of accuracy is consistent with a previous work that has shown that LiDAR ground returns can be used to detect very subtle geomorphic gradients in wetland environments (Richardson *et al.*, 2010). The average topographic gradient for the study site was determined to be approximately 0.1% on the basis of the regional change in elevation captured by the LiDAR survey.

Landscape analysis

Landscape analysis was conducted to assess whether temporal changes in the *Q–GDA* analysis could be explained on the basis of differences in catchment geomorphology and scale. Although the LiDAR acquisition did not cover all six of the gauged research catchments, it captured a sufficiently large area such that it could be used to conduct quantitative geomorphic analyses across a range of scales assumed to be representative of the six research catchments. A digital stream network was used as a

sampling template to analyse geomorphic gradients at multiple scales (based on stream order) along the drainage network. The network was derived from the 5-m LiDAR DEM using SAGA (System for Automated Geoscientific Analysis) GIS (Olaya and Conrad, 2009). Streams were initiated from a Strahler order grid, which are sometimes more precise than using a minimum contributing area as a criteria for initiating channels (Olaya and Conrad, 2009). A minimum Strahler value of 5 was used, and only segments greater than 1000 m were kept. Note that, at this initial stage, Strahler order values refer to pixel convergences, not streams. The result was a digital stream network that matched those streams that were clearly visible in a 0.5-m resolution pan-sharpened IKONOS image available over the same footprint as the LiDAR survey. Many streams were too narrow or obstructed by vegetation to be visible in the IKONOS image, thus requiring some manual interpretation of flowpaths based on the imagery and field reconnaissance. Importantly, streams in this context were interpreted quite broadly, representing both perennial and ephemeral stream channels, as well as potential overland flowpaths likely only to be active during very wet periods and typically corresponding to fen water tracks visible within the IKONOS imagery. Streams segments that did not originate entirely within the LiDAR footprint were excluded from the analysis as the assigned stream order would be inaccurate. Also excluded were any segments deemed to be influenced by built-up areas associated with the Victor mine site or that were emptying into much larger order river systems and

therefore whose geomorphology could be influenced strongly by the larger system, as in the case of all tributaries flowing into the Attawapiskat River. For all subsequent analyses, a Shreve stream ordering system was used to give a more continuous and higher precision representation of scale increases along drainage networks compared with the more conventional Strahler ordering system. In the Shreve system, stream order n increases with each successive tributary entering the system, whereas Strahler order only increases when two streams of the same order join to form a third stream of order $n+1$. The stream segments ranged from Shreve order 1 to 7 (whereas Strahler orders only ranged from 1 to 4, which is a comparative loss of precision for subsequent analyses described). In total, 57 stream segments were considered suitable for further analysis (Figure 2). The *GDA*s associated with each of these 57 segments spanned a range of 1–40 km^2 (Figure 3). Tributaries 3, 5 and 7 are all larger than 40 km^2, which represents a limitation of the geomorphic analyses in this study because of the available extents of the LiDAR survey. The fact that a Strahler order grid was used for initiation of the digital stream network was not relevant to the ultimate decision to use a Shreve ordering system in the subsequent analysis and simply reflects the nature of the GIS algorithms available for stream network delineation within the software environment.

Three analyses were conducted using the derived streams as sampling units. The first two were accomplished by sampling DEM derivatives within a fixed buffer zone of
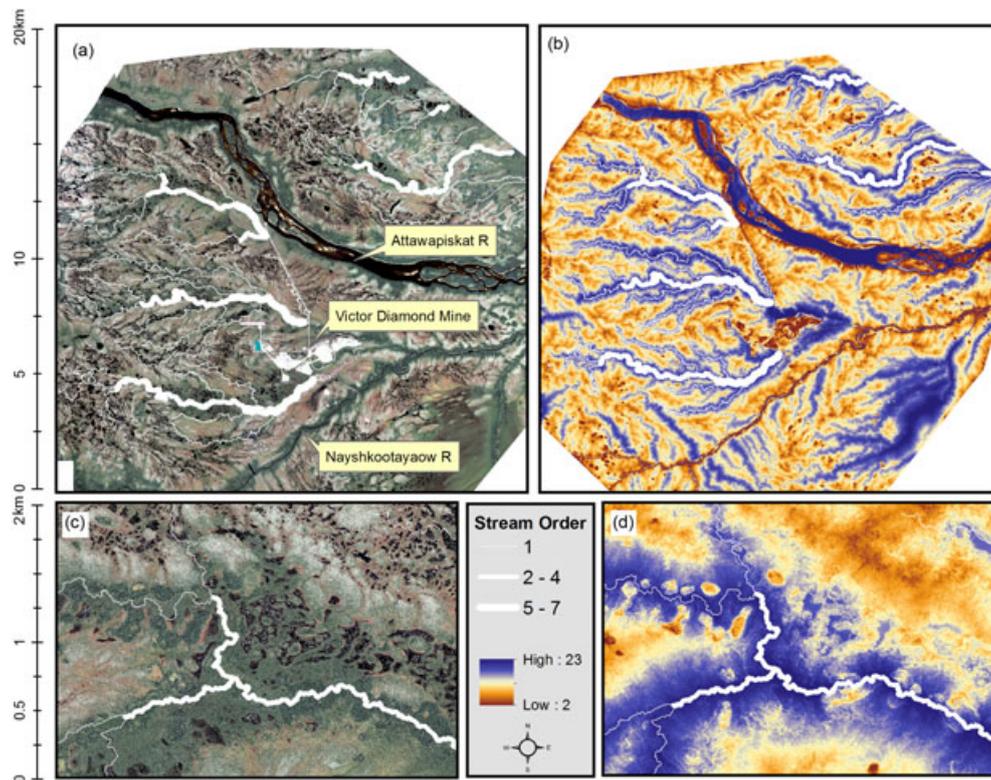

Figure 2. LiDAR digital elevation model (DEM)-derived stream network overlaying (a) IKONOS imagery and (b) *SWI* grid computed from LiDAR DEM. Larger scale insets are also shown (c, d). Note the strong spatial agreement between channel fens (dark green areas) in IKONOS image (c) and higher *SWI* values (d)
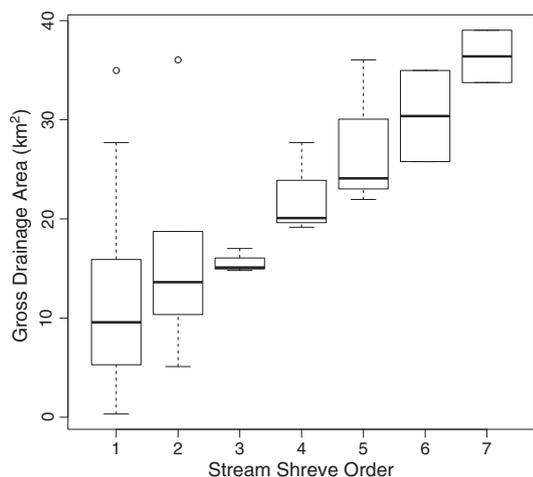
Figure 3. Distribution of stream segment gross drainage areas falling within the LiDAR survey footprint, by Shreve order

150 m surrounding each individual stream segment. The DEM derivatives sampled were the gradient and the length over gradient (*L/G*) index, computed at each pixel relative to the nearest downslope stream segment (Figure 4a). Both gradient and *L/G* are derived from the vertical distance to channel network (*VDCN*) and horizontal overland flowpath distance to channel network (*HOFDCN*) functions in SAGA. Gradient (*G*) is calculated as *VDCN/HOFDCN*, and *L/G* is calculated as *HOFDCN/G*. The *L/G* index in this case is a topographically derived proxy for flowpath transit time from any given pixel to the nearest stream (Richardson *et al.*, 2009). Both the *G* and *L/G* indices were computed for each pixel within the fixed buffer zone and an average computed from the distribution extracted for each stream segment (Figure 4a).

The purpose of the third and final analysis was to assess the spatial distribution of a modified topographic wetness index (*TWI*) along the drainage network. More specifically, it was to quantify scale-dependent variations in the width of near-stream zone runoff generating areas inferred from the wetness index. The modified *TWI* was calculated on a pre-processed version of the 5-m LiDAR DEM using SAGA. The traditional *TWI* calculation is problematic in lowland environments because it does not adequately account for extensive lateral dispersion of

water that occurs in such landscapes. The SAGA wetness index (*SWI*) is formulated to account for this dispersion through an iterative process that distributes calculated contributing area values between pixels as a function of local slope (*β*). It uses the same formula as the traditional *TWI* (i.e. ln [specific catchment area (*SCA*)]/tan *β*}, (Beven and Kirkby, 1979)) but is based on a modified specific catchment area (*SCA_M*) calculation (Bohner and Selige, 2002) as follows:

$$SCA_M = SCA_{max}\left(\frac{1}{15}\right)^{\beta \exp\left(15^{\beta}\right)} \text{ for } SCA \quad (1)$$

$$< SCA_{max}\left(\frac{1}{15}\right)^{\beta \exp\left(15^{\beta}\right)}$$

$$SWI = \ln\left(\frac{SCA_M}{\tan\beta}\right) \quad (2)$$

Specific catchment area can be considered equivalent to *GDA* for any point in the landscape, whereas the *SCA_M* is a locally modified value of *SCA*, which is iteratively calculated via a focal neighbourhood operator until the condition in (1) is satisfied (if the condition in (1) is initially satisfied, no modification is implemented). This effectively disperses the *GDA* across all pixels within localized flat areas such that at any given value cannot be directly interpreted as the *GDA* for that location. The calculated *SWI* layer for the entire LiDAR DEM used in this study is shown in Figure 2. The subsequent analysis on the *SWI* layer made use of the threshold buffer algorithm in SAGA GIS. This algorithm uses a DEM and a second geomorphic index raster layer to grow a contiguous connected area outwards from a defined target feature, in this case a single segment of the digital stream network, until a user specified threshold in the geomorphic index is no longer exceeded. This is carried out on a pixel by pixel basis, such that only pixels that satisfy the threshold criteria and that are connected to the stream reach by a contiguous sequence of pixels that also meet the threshold criteria are included in the result. For each reach, a near-stream zone was then calculated on the basis of the 70th, 80th and 90th percentiles in the *SWI* layer as
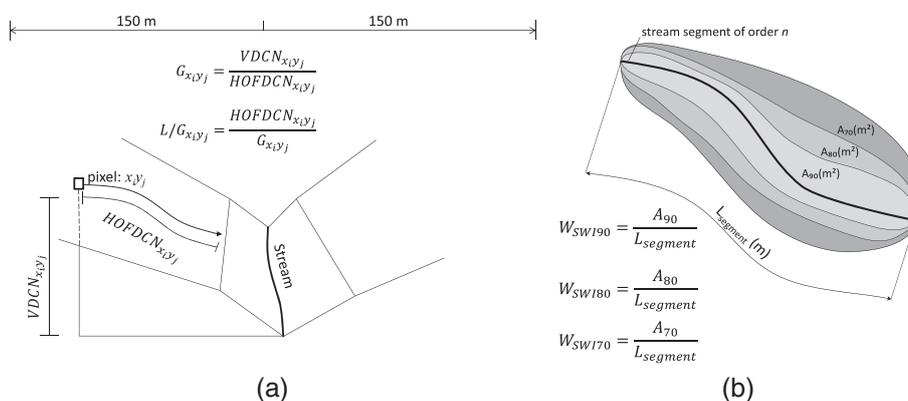

Figure 4. Schematic of geomorphic index calculations *G* and *L/G* (a) and *SWI*_{70–90} (b). *G* and *L/G* are the means of the distributions of all pixel values within a 150 m buffer zone surrounding the channel segment. *SWI*_{70–90} is the total area of contiguous pixels of *SWI* value greater than or equal to the stated *SWI* percentile (computed from the distribution for the entire LiDAR scene, Figure 2b), normalized to the stream channel length

shown in Figure 2, as an optimal threshold could not be determined *a priori*. The area of each near-stream zone was calculated and divided by the stream reach to give an estimate of the nominal width of these potential hydrologic contributing areas (Figure 4b).

RESULTS

Total rainfall during the study period was 492 and 354 mm for 2009 and 2010, respectively. These totals and all subsequent analyses are for the growing seasons only, from May 5 to October 17 of each year. A substantial proportion of the 2010 rainfall occurred in July, and prior to that, the conditions were exceptionally dry following the 2009/2010 winter with very low snowfall and a non-existent snowpack just prior to the normal melt period. The average runoff from the six research catchments was 420 mm in 2009 and 134 mm in 2010 (Table I), representing runoff coefficients of 0.85 and 0.38, respectively. In both years, total runoff contributions during flow periods exceeding the 90th percentile represented approximately 30% of the total observed growing season runoff. Conversely, contributions during low flow periods ($\leq$10th percentile) were just 2–3% (Table I). The results of the daily *Q versus GDA* analysis for 2009 and 2010 (i.e. daily coefficient of determinations or R^2), along with the runoff hydrographs for each of the six catchments, are provided in Figure 5. Average R^2 were 0.95 in 2009 and 0.92 in 2010. In both years, therefore, *GDA* explained a very high proportion of total observed differences in discharge among the six catchments. The distributions of R^2, however, were negatively skewed, and the minimum calculated R^2 was 0.47 in 2009 (wet year) *versus* 0.79 in 2010 (dry year). In 2009, large decreases in R^2 coincided very closely with periods of quickflow runoff generation (hydrograph peaks). Days for which total runoff was most proportional among basins occurred during baseflow periods, and this is when the *Q–GDA* relationships were the strongest based on the magnitude of the R^2 coefficient (Figure 5).

Daily runoff values are summarized by catchment, year and flow conditions in Figure 6 and in Table I. For all but the largest catchments (e.g. Trib 5, 204 km^2), there was a tendency for runoff to increase with increasing drainage area during higher flow periods (Figure 6a). This is most noticeable at high flow conditions (daily runoff $\geq$90th percentile) in 2009 (Figure 6c) and to a lesser extent during mid (55th to 65th percentile) and low ($\leq$10th percentile) flows of the same year. Many of the observed differences between catchments were statistically significant ($p \leq 0.05$) on the basis of Wilcoxon matched pairs test, and these results consistently corroborated the visual difference of medians test that can be accomplished by comparing the notches (tapered portions of boxplots) on any pair of boxplots in a panel. Results of these difference tests are provided for 2009 and 2010 totals in Table II. Total growing season runoff in 2009 (Figure 6d) mirrored the daily flow boxplots during high flow periods (Figure 6c). In 2010, differences between catchments were large, but total runoff was very low, and in contrast to 2009, there were no relationships with catchment size (Figure 6f, g). Differences in total runoff among catchments during the 2009 growing season (Figure 6h) were negligible, with no discernible pattern as a function of scale.

LiDAR-derived metrics of near-stream zone morphology (mean gradient) showed clear and consistent differences among stream segments of different Shreve order, used here as a measure of catchment scale (Figure 7). This relationship was moderate but significant ($R^2 = 0.43$, $p < 0.01$). The *L/G* index decreased with increasing Shreve order (Figure 6b), a relationship that was also moderate but significant ($R^2 = 0.4$, $p < 0.05$). The *SWI* analysis also demonstrated consistent morphological changes across scale in this landscape whereby nominal width of *SWI*-defined near-stream zones increased with increasing stream order (Figure 8). However, there was a threshold Shreve order of about 4, beyond which the nominal width appeared to fluctuate somewhat, probably because of the lower number of stream segments in the these Shreve order classes.

Table I. Summary of total runoff by catchment for 2009 and 2010 growing season, and total runoff contributions during low ($\leq$10th percentile), medium (55–65th percentile) and high ($\geq$90th percentile) flow conditions

Catchment	Area (km^2)	2009 Total runoff (mm)	2009 Total runoff (mm) in flow percentile class 0–10%	55–65%	90–100%	2010 Total runoff (mm)	2010 Total runoff (mm) in flow percentile class 0–10%	55–65%	90–100%
Trib 5	204	413	12	36	116	154	3.1	11	51
Trib 3	127	549	12	39	212	102	2.6	10	27
Trib 7	51	559	17	51	165	162	3.8	15	53
Trib 5a	30	406	16	35	123	112	3.2	9	34
SNGC	21	337	12	28	78	127	3	16	26
NNGC	9	258	12	25	51	144	2.4	16	29
Mean		420	14	36	124	134	3	13	37
% of flow			3	8	30		2	10	27

Percentiles were calculated from the regional mean daily runoff for each year.
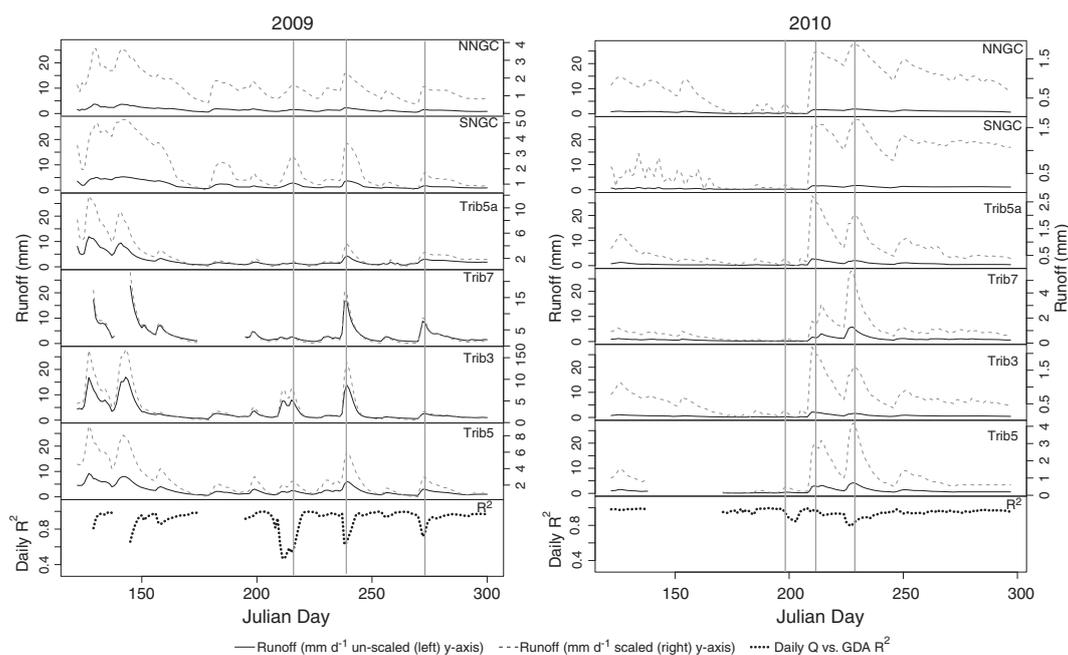NNGC, North-North Granny Creek; SNGC, South-North Granny Creek.

Figure 5. Daily *Q versus GDA* analysis for 2009 and 2010 growing seasons. The solid black lines show runoff in mm day^{-1} on the unscaled (left) *y*-axes. To facilitate visual identification of runoff events, the same data are shown on the scaled (right) *y*-axes using the dashed grey line. Vertical lines are provided to facilitate comparisons of runoff timing for several of the largest events

DISCUSSION

Temporal dynamics of the Q versus GDA relationship

Recent studies have shown that hydrologic dynamics and connectivity of spatially isolated storage elements (namely lakes and wetlands) can strongly affect the temporal dynamics of catchment runoff efficiency because of large variations in the proportion of hydrologically effective areas (i.e. those parts of the catchment that are actively generating runoff and also hydrologically connected to the outlet, Woo and Mielko, 2007; Spence *et al.*, 2010; Phillips *et al.*, 2011). There is also evidence to suggest that connectivity and storage dynamics of discrete response units influence hydrologic efficiency in northern peatland catchments, at least over small length scales. For example, past work by Quinton and Roulet (1998) demonstrated that within a subarctic fen (at a scale of $<1\,\text{km}^2$), variations in pool-ridge hydrologic connectivity was a first-order control on runoff response of the wetland. Hydrologic connectivity in northern peatlands at larger catchment scales (e.g. 10 to $100\,\text{km}^2$), however, has not been well studied. In particular, it is unclear whether landscape unit connectivity over larger peatland basins operates in a manner consistent with the fill-and-spill conceptual model of runoff generation that has recently gained some prominence within the hydrologic research community (Tromp-van Meerveld and McDonnell, 2006; Woo and Mielko, 2007; Spence, 2010).

It is within this broader context that the results of this study are interpreted. We anticipated large temporal variations in the strength of the *Q–GDA* relationship as a manifestation of inter-catchment differences in runoff timing and/or hydrologic efficiency caused by differences in catchment scale and/or temporal discontinuities in the proportion of active and contributing areas among the six research catchments. In regions where landscape element thresholds dictate hydrologic efficiency of catchment systems by regulating the proportion of active contributing areas, runoff generation should become most proportional during high flow conditions (i.e. strongest *Q–GDA* relationships). In relatively disorganized and heterogeneous drainage systems typical of Precambrian Shield landscapes, the rate at which active and contributing areas become connected or disconnected during drier flow periods should vary considerably and somewhat unpredictably across the landscape, and this could create a condition where different catchments generate disproportionate amounts of runoff at any given time. We posited that this would lead to a breakdown in the *Q–GDA* relationship during dry periods over the study period. Alternatively, in a system dominated by spatial patterns of runoff more typical of the VSA model, temporal characteristics of the *Q–GDA* relationship could differ considerably. A key assumption of the VSA theory is that of linear wetting and drying from near-stream zones upwards through the hillslope towards the catchment divide (McDonnell, 2003). This continuous, linear expansion away from streams implies that connected, active areas may expand and contract in response to wetness conditions with some degree of proportionality among different watersheds within a region, particularly if the drainage network is well organized. In this situation, a plausible characteristic of the *Q–GDA* relationship over time is one that is relatively temporally invariant or that changes primarily in response to differences in runoff timing along the drainage network (e.g. because of scale-related differences in channel routing). On the basis of the analysis presented in this study and interpretations in the following section, we suggest that the VSA concept is applicable in this low gradient landscape because of its well-organized drainage structure and strong potential for dynamic, linear expansion and contraction of near-stream zone hydrologic source areas.
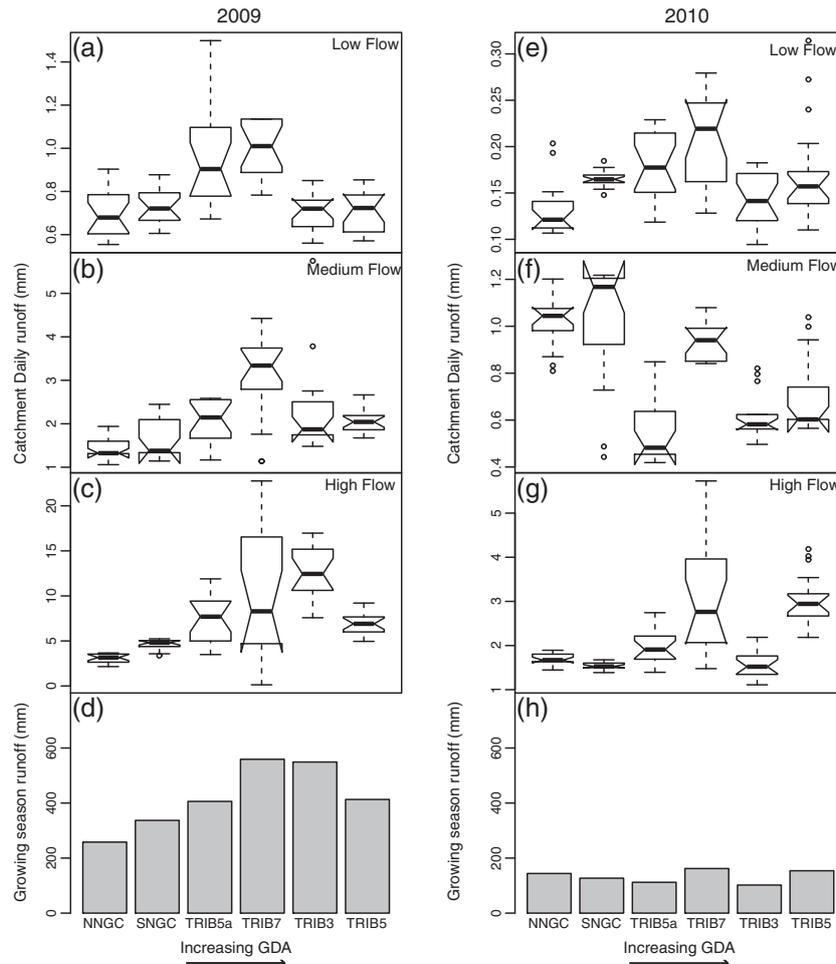
Figure 6. Daily runoff summarized for each catchment at low (≤10th percentile), medium (55th to 65th percentile) and high (>90th percentile) flow conditions (based on mean daily runoff of all six catchments) for 2009 (a–c) and 2010 (e–g) and total growing season runoff by catchment for 2009 (d) and 2010 (h). Flow conditions are shown in the upper right corner of each panel and indicate that the boxplots represent daily runoff only for days falling within the specified flow period. In these plots, catchment size increases from left to right (refer to Table I). Boxplots show the median, inter-quartile range, range and outliers. Non-overlapping notches (tapered sides) between any pair of boxplots indicate that the respective medians are significantly different at the 95% confidence level (R Development Core Team, 2009). Statistical significance of the between-catchment differences in total runoff in 2010 (d) can be inferred from the paired Wilcoxon test results for daily runoff (Table II). Note the differences in the *y*-axis scales

Table II. Wilcoxon matched pairs tests of daily runoff differences for catchment pairs for 2009 (lower right) and 2010 (upper right). The absolute value of the difference in total observed runoff is shown along with the *p*-value (in parentheses) resulting from the statistical test (significant test results shown in bold for 95% confidence interval)

	Trib 5	Trib 3	Trib 7	Trib 5a	SNGC	NNGC
Trib 5	—	**51 mm (<0.001)**	8 mm (0.20)	**42 mm (0.001)**	27 mm (0.61)	10 mm (0.11)
Trib 3	136 mm (0.86)	—	**59 mm (<0.001)**	9 mm (0.91)	**24 mm (0.02)**	**41 mm (<0.001)**
Trib 7	**146 mm (0.04)**	10 mm (0.10)	—	**49 mm (<0.001)**	35 mm (0.52)	18 mm (0.29)
Trib 5a	7 mm (0.18)	143 mm (0.15)	**153 mm (0.02)**	—	15 mm (0.10)	**32 mm (<0.001)**
SNGC	**76 mm (0.02)**	**212 mm (0.01)**	**154 mm (<0.01)**	68 mm (0.37)	—	17 mm (0.30)
NNGC	**155 mm (<0.001)**	**291 mm (<0.001)**	**302 mm (<0.001)**	**148 mm (0.01)**	79 mm (0.12)	—

SNGC, South-North Granny Creek; NNGC, North-North Granny Creek.

Sources of Q–GDA model errors during high flow periods

Initially, spatial variability of precipitation was considered as a possible source of the breakdown in the *Q–GDA* relationship during runoff events. However, the climate in this region is moderated by Hudson Bay, and isolated convective systems are unlikely to have caused sufficiently large short to medium term differences in precipitation inputs among the watersheds that would have caused the observed *Q–GDA* model errors during high flow periods. We plotted the cumulative daily precipitation (not shown) recorded at Lansdowne House (located 200 km west, which is the prevailing wind direction) for June, July and August of 2009 and 2010 *versus* the weather station in the study area. Total precipitation varied by less than 5% and offered exceptional agreement through time, supporting our
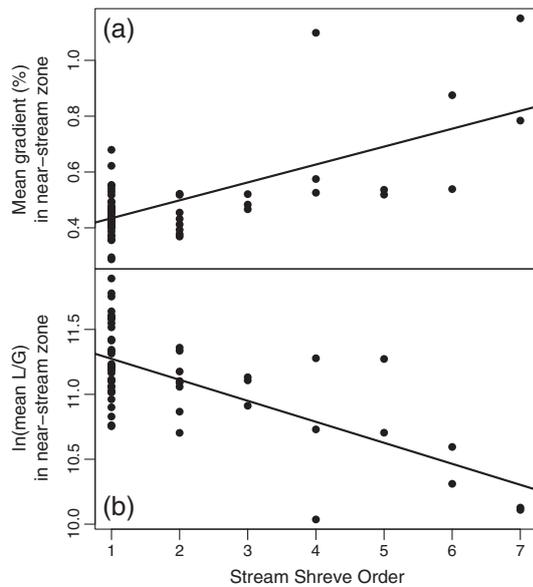
Figure 7. Relationship between Shreve order and (a) mean gradient and (b) *L/G* in the near-stream zone defined by a 150 m linear buffer around each stream segment
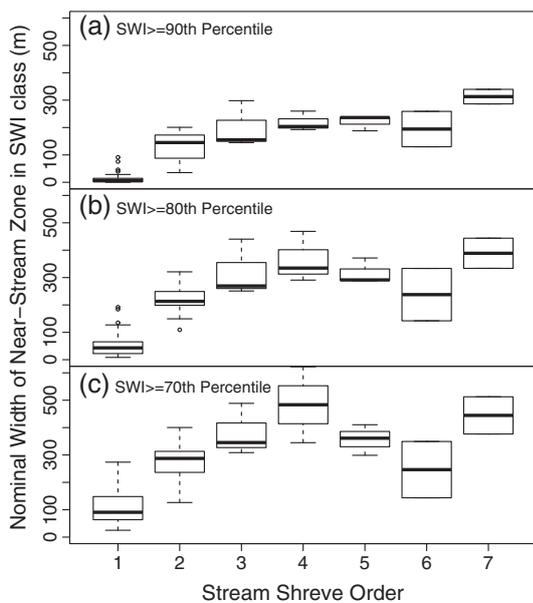

Figure 8. Relationship between Shreve order and the nominal width of near-stream zones defined by *SWI* threshold buffers. Percentiles indicate the *SWI* threshold used to define the near-stream zone and are based on the distribution of the entire *SWI* image (Figure 2b)

assumption that isolated convective systems were probably not responsible for the observed deviations from the *Q–GDA* relationships, at least during the largest events where runoff responses were observed for all six catchments. In addition, we found that systematic differences in total runoff (mm) among the catchments drove the pattern of increasing model errors during high flow periods, and these differences were sustained throughout events (i.e. were not caused by short-term differences in runoff timing caused by scale-dependent effects such as routing lags). A number of discrete runoff events in 2009 and 2010 show that timing of peak flows and recessions were normally very coincident across the six catchments and not a probable source of

Q–GDA model errors (Figure 5). In 2009, the smallest catchments had the lowest total runoff, implying that they diverted a greater proportion of precipitation inputs into outputs of either evaporation or groundwater recharge pathways, rather than runoff. In 2010, which was a much drier year, there was little to no systematic variation with scale nor was there any consistency in the observed inter-catchment differences during low, medium and high flow conditions (Table I, Figure 6e–g). As a result, total runoff for the 2010 study period was very consistent among all six watersheds (Figure 6h). The hydrometric responses across the six catchments in this study therefore show that the systematic breakdown of the *Q–GDA* relationship during higher flow conditions was primarily attributable to differences in runoff efficiency rather than runoff timing. We attribute the increase in runoff efficiency with increasing catchment size and wetness conditions to the subtle but systematic changes in near-stream zone geomorphology (increasing width and gradient, decreasing *L/G*, as seen in Figures 7 and 8), which likely become more important during high flow conditions because of stronger topographic control of lateral flow during high flow periods.

Geomorphology and runoff response

Quantitative geomorphology provides a means to link landscape pattern to process (Fisher *et al.*, 2007) and is central to much past and current research in catchment hydrology and hydrologic modelling (Anderson and Burt, 1978; Troch *et al.*, 1995; McGlynn and McDonnell, 2003; Jencso *et al.*, 2009). The geomorphic characteristics of a catchment represent the equilibrium response of the landscape to historical climate conditions over timescales of centuries to millennia but imparts a first-order control on contemporary runoff response (Beven and Kirkby, 1979). Geomorphic form is intricately linked to ecohydrological feedbacks driving northern peatland development (Glaser *et al.*, 2004), and strategic landscape analysis with high resolution imagery can lead to new insights into the hydrology of these important northern ecosystems, as demonstrated by the use of airborne LiDAR in the present study.

LiDAR surveys offer unprecedented detail for linking geomorphic patterns and processes in peatland ecosystems (Richardson *et al.*, 2010). The three LiDAR DEM-derived indices presented here provide a quantitative description of near-stream zone geomorphology in an HBL peatland complex. Landscape structure varied predictably with scale, and these variations were consistent with the observed, scale-dependent variations in runoff generation during high flow periods. Specifically, near-stream zone gradients increased with increasing Shreve order, and the *L/G* index of lateral transit times (flowpath length normalized by gradient) decreased. Near-stream zones of elevated *SWI* became wider with increasing stream order, despite concurrent increases in gradient that should effectively lower the calculated *SWI* in these areas. This reflects the fact that contributing area influences the spatial variation in *SWI* more strongly than slope in this landscape. Higher *SWI* implies wetter conditions and the potential for a water table that is closer to the ground

surface, which, combined with steeper gradients, can produce rapid lateral transmission of water to the stream network. The spatially discrete near-stream zone areas, quantified using a threshold buffer on the *SWI* image, probably contribute strongly to the quickflow response and are a plausible source of the observed breakdown in the *Q versus GDA* relationship at high flows and increased runoff from the larger catchments in the 2009 growing season. Also, the highest *SWI* values in the LiDAR imagery (Figure 2b) correlate well with channel fen areas in the IKONOS image (Figure 2a), at least qualitatively. Channel fens are darker green areas in the IKONOS imagery, and manual interpretation has been confirmed at the study site through field reconnaissance. Therefore, the areal distribution of *SWI* and its tendency to increase with increasing stream order is likely a proxy for downstream increases in the aerial proportions of channel fens along the drainage network.

Wetness indices such as the *TWI* and *SWI* are widely regarded for their ability to quantitatively describe spatial variability of runoff generating areas (Beven *et al.*, 1988). The *SWI*, which modifies the traditional *TWI* calculation by accounting for lateral dispersion of water in very flat areas, is particularly promising for applications in northern peatlands. Further work is required to assess the potential to use this index with coarser resolution DEM products that are more widely available.

Runoff generation across scales

Overall, our analyses of daily runoff under different flow conditions and between years demonstrate that runoff efficiency diverged systematically among the watersheds at high flows, and these differences resulted in large and statistically significant differences in total runoff in the wetter growing season of 2009. In 2010, differences in runoff among the catchments were significant but not large or consistent across the range of flows, resulting in similarly low amounts of runoff among the six catchments (Figure 6h). Furthermore, during high flow periods in 2009, total runoff increased systematically with increasing catchment area up to a catchment size of about 50 km^2 (Trib 7) and then decreased successively for the two final increases in scale (Trib 3 and Trib 5) (Figure 6d). For Trib 5, the largest catchment at 204 km^2, total runoff in 2009 was approximately equivalent to the average of the five smaller catchments. Often, there is a critical catchment size, termed the representative elementary area (REA), beyond which variability in runoff response with scale is much reduced because of the tendency for larger catchments to average the smaller scale variations in local runoff generating processes and/or landcover proportions (Wood *et al.*, 1988). The REA is a useful scaling metric because it can potentially be used to determine the extent to which explicit treatment of watershed composition and configuration is required in numerical modelling efforts. The fact that total runoff from Trib 5 during the 2009 growing season was similar to the average of the other five smaller catchments (Figure 6a–c) provides some preliminary evidence for a REA of approximately 200 km^2 in this region in order to integrate scale-dependent differences in runoff efficiency during high

flow conditions. In Figure 8, there appears to be a scaling break around Shreve order 4 (or approximately 20–30 km^2 beyond which the near-stream zone width plateaus) or begins to decrease with further increases in stream order (Figure 8a–c). A catchment area of 200 km^2 may be sufficient to integrate these scale-dependent variations in near-stream zone geomorphology, thus leading to the observed runoff response during the wetter (2009) growing season that was similar to the average of the remaining five catchments. During the drier growing season of 2010, the REA may be less relevant, as runoff generation was much more proportional across the six catchments. Note that this preliminary REA suggestion can only be considered applicable for the range of scales analysed (i.e. medium to large headwater catchments in this landscape with *GDA*s ~200 km^2 over seasonal times scales) and may have differed had we considered even larger catchments or shorter/longer time scales. Further efforts are therefore required to assess whether this finding holds across a broader range of scales and to explicitly quantify potential scale-dependent variability in runoff, landcover and geomorphology.

Landscape organization and geomorphology in northern peatland complexes

Although it was restricted to the headwater catchment scale due to the extents of the LiDAR survey, the landscape analysis reported here points to some intriguing questions about landscape evolution in northern peatland complexes. The fact that W_{SWI80} and W_{SWI70} began to decrease beyond a Shreve order of 4 (Figure 8b and c) suggests a reversal of the observed trends in *SWI* width indices with further increases in catchment scale. This is also a plausible cause of the observed trend reversal in runoff generation beyond a *GDA* of 50 km^2. Larger order systems within the LiDAR footprint are consistently more incised and have distinctly lower *SWI* signature in their immediate vicinities. For example, the Nayshkootayaow River (Figure 2a) can be seen running from the southwest to northeast in the southern half of the IKONOS imagery and *SWI* layer (Figure 2a and b). In the *SWI* layer, this river lacks the distinctive near-stream zone of high *SWI* values surrounding the channel, as seen in the lower-order stream segments. Peatlands are aggrading ecosystems that exhibit geomorphologic characteristics consistent with self-adapting mechanisms that maximize water optimization (Clymo, 1984). For example, the low permeability catotelm delays lateral runoff and inhibits vertical seepage losses (Ingram, 1978), whereas the higher permeability of the acrotelm reduces the duration of surface flooding during snowmelt and following large precipitation events (Spieksma, 1999). Peatlands modify horizontal gradients through ecohydrological feedbacks driving rates of peat accumulation and decomposition (Glaser *et al.*, 2004). Our observation of lower near-stream zone gradients in smaller order systems is consistent with these notions of peatland development. The lower gradient/lower *SWI* areas coincide with bog-dominated portions of the research catchments. With increasing drainage area and hence stream order, steeper gradient channel fens become more promin-

ent, which is consistent with their imperative to shed accumulated water from upslope areas, particularly during wet periods. With further increases in stream order, there is a potential shift away from ecohydrological feedbacks (aggradational) contributing to peat accumulation towards fluvial geomorphologic feedbacks (erosional) driving channel form, which would result in more incised channels and narrower SWI_{70-90} width indices. The HBL region therefore presents an interesting case study for future research on the differential roles of aggradational *versus* erosional regimes in driving landform evolution in northern peatland basins.

CONCLUSION

Runoff generation is a multi-scale phenomenon, and previous field research has shown that examining relationships between catchment size and streamflow characteristics can help us understand spatial and temporal characteristics of hydrologic source areas (Wood *et al.*, 1988; McGlynn *et al.*, 2004). Despite many recent advances in physical hydrology of northern peatlands (Waddington *et al.*, 2009), it remains difficult to translate our process-based hydrologic understanding of peatland catchments into simple but reliable conceptual and numerical models of water flow through these landscapes. Moreover, it remains unclear how the widely accepted conceptual model of 'partial contributing areas' (Betson, 1964) might apply to northern peatland catchments. This issue is of particular relevance now given accumulating evidence that partial contributing areas do not necessarily expand and contract along drainage networks in continuous fashion, as described in much of the classic and ensuing literature on the topic (Engman, 1974; McDonnell, 2003). Rather, a new conceptual model suggests that storage dynamics in discrete and spatially isolated landscape features dictate partial area contributions within catchments, and this is thought to be of particular relevance in northern landscapes dominated by lakes and wetlands (Spence, 2010).

Accordingly, this paper presents a new approach for examining first-order controls on runoff generation across scales on the basis of a case study of six northern peatland basins ranging in size from 9 to 204 km². A daily Q *versus* GDA analysis was used to identify potential times where hydrologic efficiency diverged among catchments of different size, and several high resolution geomorphic indices were quantified and found to vary predictably with scale. On the basis of these two sets of analyses, we propose that observed differences in runoff generation were driven by differences in the size and geomorphologic characteristics of near-streams zones, regions most likely dominated by channel fens and fen water tracks. We conclude with the following summary of our findings and interpretations:

1. In the six headwater research catchments, runoff efficiency increased with catchment size at high flows up to a scale of 50 km² and then decreased with further increases in catchment size up to 200 km², the largest

catchment analysed. This behaviour resulted in reductions in the strength of the relationship between Q and GDA. At low flows, runoff generation did not vary systematically across scale, resulting in very strong relationships between Q and GDA.

2. Across the range of catchment scales analysed, near-stream zone geomorphology of ephemeral and perennial streams and flowpaths exhibited structural organization, as elucidated by the lateral flowpath gradients (increasing with stream order), the L/G index of lateral transit times (decreasing with stream order) and the nominal width of potential runoff contributing areas modelled by the SWI (increasing with stream order to a point and then decreasing).

3. Interpreted together, conclusions 1 and 2 imply that smaller order headwater systems in this landscape partition more precipitation into storage and evaporative pathways, resulting in lower area-normalized water yields.

4. Fast-responding flowpaths in the spatially discrete near-stream zones are potentially a key determinant of catchment runoff efficiency. The importance of these critical source areas likely increases with increasing wetness, consistent with the well-known VSA concept of runoff generation.

5. Peatlands are complex adaptive systems, and the structural organization reported here likely reflects the influence of both ecohydrological and geomorphologic feedback mechanisms. The fact that the trends of increasing runoff (at high flow) and increasing SWI width index reversed beyond a threshold catchment scale could imply that there is a critical catchment scale beyond which the drainage network switches from an aggradational regime dominated by ecohydrological feedbacks to an erosional regime dominated by fluvial geomorphological feedbacks.

The HBL is one of the largest peatland complexes in the world and is entering a period of unprecedented ecological change due to anthropogenic impacts on land use and global climate. This study presents new findings on the influences of geomorphology and scale on runoff generation in a northern peatland complex within a region of global ecological significance. Our results imply that further research into landscape organization and its underlying ecohydrological and geomorphologic drivers will help lead to a more informed understanding of the relative merits of VSA *versus* storage-threshold (fill-and-spill) conceptual models of runoff generation in northern lowland regions. Future research will benefit from incorporating these insights into predictive hydrological modelling efforts focused on ungauged peatland basins of Canada and other northern peatland dominated regions of the world including Alaska, northern Europe and western Siberia.

REFERENCES

Anderson M, Burt T. 1978. The role of topography in controlling throughflow generation. *Earth Surface Processes* 3(4): 331–344.

Betson RP. 1964. What is watershed runoff? *Journal of Geophysical Research* 69(8).

Beven KJ, Kirkby MJ. 1979. A physically-based, variable contributing area model of basin hydrology. *Hydrological Sciences Bulletin* 24(1): 43–69.

Beven KJ, Wood EF, Sivapalan M. 1988. On hydrological heterogeneity – catchment morphology and catchment response. *Journal of Hydrology* 100(1–3): 353–375.

Bohner J, Selige T. 2002. Spatial prediction of soil attributes using terrain analysis and climate regionalization. *Gottinger Geograpihsche Abhandlungen* 115(13–28).

Buttle JM, Eimers MC. 2009. Scaling and physiographic controls on streamflow behaviour on the Precambrian Shield, south-central Ontario. *Journal of Hydrology* 374(3–4): 360–372.

Clymo R. 1984. The limits to peat bog growth. *Philosophical Transactions of the Royal Society of London. B, Biological Sciences* 303(1117): 605.

Damman AWH. 1986. Hydrology, development, and biogeochemistry of ombrogenous peat bogs with special reference to nutrient relocation in a western newfoundland bog. *Canadian Journal of Botany-Revue Canadienne De Botanique* 64(2): 384–394.

Engman ET. 1974. Partial area hydrology and its application to water resources. *Water Resources Bulletin* 10(3).

Environment Canada. 2003. Canadian Climate Normals or Averages 1971-2000. Environment Canada. http://climate.weatheroffice.gc.ca/climateData/canada_e.html (Accessed 2011).

ESRI. 2011. ArcGIS Desktop: Release 10.0 Redlands, CA: Environmental Systems Research Institute.

Fisher SG, Heffernan JB, Sponseller RA, Welter JR. 2007. Functional ecomorphology: feedbacks between form and function in fluvial landscape ecosystems. *Geomorphology* 89(1–2): 84–96.

Gagnon AS, Gough WA. 2005. Trends in the dates of ice freeze-up and breakup over Hudson Bay, Canada. *Arctic* 58(4): 370–382.

Glaser PH, Hansen BCS, Siegel DI, Reeve AS, Morin PJ. 2004. Rates, pathways and drivers for peatland development in the Hudson Bay Lowlands, northern Ontario, Canada. *Journal of Ecology* 92: 1036–1053.

Gough WA, Wolfe E. 2001. Climate change scenarios for Hudson Bay, Canada, from general circulation models. *Arctic* 54(2): 142–148.

Ingram H. 1978. Soil layers in mires: function and terminology. *European Journal of Soil Science* 29(2): 224–227.

Jencso KG, McGlynn BL, Gooseff MN, Wondzell SM, Bencala KE, Marshall LA. 2009. Hydrologic connectivity between landscapes and streams: transferring reach-and plot-scale understanding to the catchment scale. *Water Resources Research* 45.

McDonnell JJ. 2003. Where does water go when it rains? Moving beyond the variable source area concept of rainfall–runoff response. *Hydrological Processes* 17(9): 1869–1875.

McGlynn BL, McDonnell JJ. 2003. Quantifying the relative contributions of riparian and hillslope zones to catchment runoff. *Water Resources Research* 39(11): 1310.

McGlynn BL, Seibert J. 2003. Distributed assessment of contributing area and riparian buffering along stream networks. *Water Resources Research* 39(4).

McGlynn BL, McDonnell JJ, Seibert J, Kendall C. 2004. Scale effects on headwater catchment runoff timing, flow sources, and groundwater-streamflow relations. *Water Resources Research* 40(7).

McGlynn B, McDonnell J, Stewart M, Seibert J. 2003. On the relationship between catchment scale and streamwater mean residence time. *Hydrological Processes* 17: 175–181.

McGuire KJ, McDonnell JJ, Weiler M, Kendall C, McGlynn BL, Welker JM, Seibert J. 2005. The role of topography on catchment-scale water residence time. *Water Resources Research* 41(5).

Olaya V, Conrad O. 2009. Geomorphometry in SAGA. In *Geomorphometry: Concepts, Software, Applications*, Hengl T, Reuter HI (eds). Elsevier: Amsterdam; 293–308.

Oswald CJ, Richardson MC, Branfireun BA. 2011. Water storage dynamics and runoff response of a boreal shield headwater catchment. *Hydrological Processes* 25(19): 3042–3060.

Phillips RW, Spence C, Pomeroy JW. 2011. Connectivity and runoff dynamics in heterogeneous basins. *Hydrological Processes* 25(19): 3061–3075.

Quinton WL, Roulet NT. 1998. Spring and summer runoff hydrology of a subarctic patterned wetland. *Arctic and Alpine Research* 30(3): 285–294.

Quinton WL, Hayashi M, Pietroniro A. 2003. Connectivity and storage functions of channel fens and flat bogs in northern basins. *Hydrological Processes* 17(18): 3665–3684.

R Development Core Team. 2009. R: a language and environment for statistical computing. R Foundation for Statistical Computing.

Richardson MC, Fortin MJ, Branfireun B. 2009. Hydrogeomorphic edge detection and delineation of landscape functional units from LiDAR digital elevation models. *Water Resources Research* 45(10): W10441.

Richardson MC, Mitchell CPJ, Branfireun BA, Kolka RK. 2010. Analysis of airborne LiDAR surveys to quantify the characteristic morphologies of northern forested wetlands. *Journal of Geophysical Research* 115(G3).

Riley JL. 2011. *Wetlands of the Hudson Bay lowlands: A Regional Overview*. Nature Conservancy of Canada: Toronto, Ontario.

Rodriguez-Iturbe I, Valdes JB. 1979. The geomorphic structure or hydrologic response. *Water Resources Research* 18: 877–886.

Rouse WR, Woo MK, Price JS. 1992. Damming James Bay: I. potential impacts on coastal climate and the water balance. *The Canadian Geographer* 36(1): 2–7.

Singer SN, Chen CK. 2002. *An Assessment of the Groundwater Resources of Northern Ontario*. Ministry of Environment: Toronto.

Spence C. 2010. A paradigm shift in hydrology: storage thresholds across scales influence catchment runoff generation. *Geography Compass* 4(7): 819–833.

Spence C, Guan X, Phillips R, Hedstrom N, Granger R, Reid B. 2010. Storage dynamics and streamflow in a catchment with a variable contributing area. *Hydrological Processes* 24(16): 2209–2221.

Spieksma J. 1999. Changes in the discharge pattern of a cutover raised bog during rewetting. *Hydrological Processes* 13(8): 1233–1246.

Stichling W, Blackwell SR. 1958. *Drainage Area as a Hydrologic Factor on the Glaciated Canadian Prairies*. Prairie Farm Rehabilitation Administration: Regina, SK.

Thompson SE, Harman CJ, Troch PA, Brooks PD, Sivapalan M. 2011. Spatial scale dependence of ecohydrologically mediated water balance partitioning: a synthesis framework for catchment ecohydrology. *Water Resources Research* 47.

Troch PA, Detroch FP, Mancini M, Wood EF. 1995. Stream network morphology and storm response in humid catchments. *Hydrological Processes* 9(5–6): 575–587.

Tromp-van Meerveld HJ, McDonnell JJ. 2006. Threshold relations in subsurface stormflow: 2. The fill and spill hypothesis. *Water Resources Research* 42(2): W02411–W.

Waddington JM, Quinton WL, Price JS, Lafleur PM. 2009. Advances in Canadian peatland hydrology, 2003–2007. *Canadian Water Resources Journal* 34(2): 139–148.

Watters JR, Stanley EH. 2007. Stream channels in peatlands: the role of biological processes in controlling channel form. *Geomorphology* 89(1–2): 97–110.

Whitfield PH, St-Hilaire A, Kamp G. 2009. Improving hydrological predictions in peatlands. *Canadian Water Resources Journal* 34(4): 467–478.

Whittington P, Price J. 2012. Impact of mine dewatering on peatlands of the james bay lowland: The role of bioherms. *Hydrological Processes*.

Woo MK, Mielko C. 2007. An integrated framework of lake–stream connectivity for a semi-arid, subarctic environment. *Hydrological Processes* 21(19): 2668–2674.

Wood EF, Sivapalan M, Beven K, Band L. 1988. Effects of spatial variability and scale with implications to hydrologic modeling. *Journal of Hydrology* 102: 29–47.

Woods R. 2003. The relative roles of climate, soil, vegetation and topography in determining seasonal and long-term catchment dynamics. *Advances in Water Resources* 26(3): 295–309.